Articles

Homology Modeling of Human Fyn Kinase Structure: Discovery of Rosmarinic Acid as a New Fyn Kinase Inhibitor and *in Silico* Study of Its Possible Binding Modes

Dubravko Jelić,*,† Boris Mildner,† Sanja Koštrun,† Krunoslav Nujić,† Donatella Verbanac,† Ognjen Čulić,† Roberto Antolović,† and Wolfgang Brandt§

GlaxoSmithKline Research Centre Zagreb, Prilaz baruna Filipovića 29, 10000 Zagreb, Croatia, and Leibniz Institute of Plant Biochemistry, Molecular Modeling Group, Halle (Saale), Germany

Received June 15, 2006

Tyrosine phosphorylation represents a unique signaling process that controls metabolic pathways, cell activation, growth and differentiation, membrane transport, apoptosis, neural, and other functions. We present here the three-dimensional structure of Fyn tyrosine kinase, a *Src*-family enzyme involved in T-cell receptor signal transduction. The structure of Fyn was modeled for homology using the Sybyl-Composer suite of programs for modeling. Procheck and Prosa II programs showed the high quality of the obtained three-dimensional model. Rosmarinic acid, a secondary metabolite of herbal plants, was discovered as a new Fyn kinase inhibitor using immunochemical and *in silico* methods. Two possible binding modes of rosmarinic acid were evaluated here, i.e., near to or in the ATP-binding site of kinase domain of Fyn. Enzyme kinetic experiments revealed that Fyn is inhibited by a linear-mixed noncompetitive mechanism of inhibition by rosmarinic acid. This indicates that rosmarinic acid binds to the second "non-ATP" binding site of the Fyn tyrosine kinase.

Introduction

Phosphorylation is one of the fundamental mechanisms of cell signaling and regulation of cell growth, proliferation, differentiation, metabolism, neural function, etc.[1−3] Members of the kinase family of the human genome encode about 500 genes, which are called the human "kinome".[4,5] Protein kinases enable transfer of γ phosphate of ATP to specific amino acids of protein substrates (tyrosine, serine, threonine, or even histidine residues).[6] Phosphorylation of certain tyrosine residues changes the enzymatic activity of tyrosine kinases and regulates specificity for substrate binding, localization, and recruitment of downstream signaling proteins. There are two major groups of tyrosine kinases: receptor and nonreceptor tyrosine kinases. Receptor tyrosine kinases are transmembrane glycoproteins that are activated by binding of their cognate ligands, and they transduce the extracellular signal to the cytoplasm.[7,8] Nonreceptor tyrosine kinases (cytoplasmatic proteins) are important components of signaling pathways through different receptors such as receptor tyrosine kinases, G-protein coupled receptors, or T-cell receptors (TCR) on the cell surface.[2] In humans, about 90 tyrosine kinases have been discovered. Fifty-eight of them are receptor tyrosine kinases divided into 20 families, while 32 of them are nonreceptor tyrosine kinases divided into 10 protein families.[9] Many of them have similar primary structure, especially in the evolutionary well-conserved kinase domain. Human tyrosine kinase Fyn (p59^{fyn}; Proto-oncogene tyrosine-protein kinase FYN, EC 2.7.1.112)[10] is a member of the nonreceptor *Src*-family tyrosine kinases. Other members of this group are Lck, Src, Yes, Lyn, Hck, Blk, Fgr, and Yrk tyrosine kinase. One of the most important roles of Fyn kinase is its participation in T-cell signal transduction,[11,12] since it is activated after stimulation of T-cell antigen receptors.[13] ITAM sequences (immunoreceptor tyrosine activation motif) of the CD3 subunit and ζ-chain of T-cell receptors are then phosphorylated by Fyn (and/or Lck, tyrosine kinase that has partially overlapping function with Fyn).[14−17] This is the prerequisite step for ZAP-70 kinase binding to ITAM and phosphorylation of LAT[18] and SLP-76[19] adaptor proteins that enable further downstream signaling pathways. The final result of this signaling process is proliferation and differentiation of T-cells, as a consequence of overexpression of interleukine-2 (IL-2), a T-cell growth factor,[20] and other cytokines. Recent studies showed that Fyn resides in different subcellular regions of the plasma membrane, linked on the membrane via its N-terminal myristyl and palmityl residues.[21−24] While most of the Lck kinase in CD4$^+$ primary T cells is found in soluble membrane fractions, more than 98% of Fyn kinase is localized in specialized plasma membrane microdomains, termed lipid rafts.[25] Also, genetic evidence demonstrates that Fyn activation is strictly connected with T-cell receptor-induced translocation of Lck,[26,21] suggesting Fyn kinase involvement in the T-cell activation process.

This study analyzed inhibition of Fyn kinase by rosmarinic acid, staurosporine, and adenosine-5′-diphosphate (ADP) (Figure 1). Staurosporine is a potent, nonselective standard inhibitor of most tyrosine kinases[27,28] and can be used as a competitive ligand in characterization of the Fyn active site. ADP can be used both in experimental and *in silico* studies of ATP-binding sites and in competition measurements.

* To whom correspondence should be addressed: Tel: +385 1 60 51 112, fax: +385 1 60 51 091, e-mail: dubravko.x.jelic@gsk.com.
† GlaxoSmithKline Research Centre Zagreb.
§ Leibniz Institute of Plant Biochemistry.

[a] Abbreviations: ATP, Adenosine-5′-triphosphate; BLAST, basic local alignment search tools; ELISA, enzyme-linked immunosorbent assay; GOLD, genetic optimization for ligand docking; IL-2, interleukine-2; ITAM, immunoreceptor tyrosine activation motif; NMR, nuclear magnetic resonance; PDB, Protein Data Bank; rmsd, root-mean-square deviation; SCR, structurally conserved region; SVR, structurally variable region; SH, *Src* homology; TCR, T-cell receptor.

10.1021/jm0607202 CCC: $37.00
Published on Web 02/22/2007

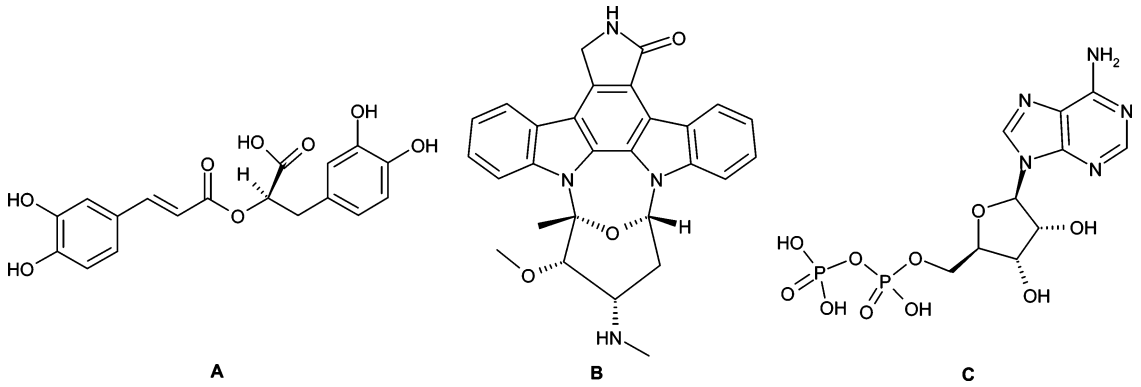

Figure 1. Chemical structures of the (A) rosmarinic acid, (B) staurosporine, and (C) adenosine-5′-diphosphate.

Figure 2. Structural organization of Fyn tyrosine kinase domains.

Table 1. Query Results of Fyn Kinase Primary Structure According to PDB Sequence Identity Search (BLASTP Search)

PDB code	protein name	% identity	*E*-values
2SRC	human tyrosine-protein kinase c-Src with AMP-PNP	77.0	6.0×10^{-134}
2PTK	chicken Src tyrosine kinase	71.7	5.3×10^{-134}
1QCF	human hemeatopoetic cell kinase with PP1 inhibitor	64.4	1.5×10^{-110}
1AD5	human hemeatopoetic cell kinase Hck with AMP-PNP	62.6	7.7×10^{-75}

Rosmarinic acid (3,4-dihydroxycinnamic acid, (*R*)-1-carboxy-2-(3,4-dihydroxyphenyl)ethyl ester) is an active ingredient of *Salvia officinalis*, *Rosmarinus officinalis*, *Prunella vulgaris*, and other plant leaves, mostly responsible for antiinfective, antiinflammatory, and antioxidative activity of these herbs.[29] Recent reports also suggest protective effects of rosmarinic acid in Alzheimer amyloid-β peptide (Aβ)-induced neurotoxicity in PC12 cells,[30] and inhibition of IKK-β (after TNF-α-induced upregulation of CCL11 chemokine, and its receptor CCR3) in human dermal fibroblasts.[31] Inhibition of T-cell antigen receptor-mediated signaling through inhibition of IL-2 promoter activation was identified as one of the mechanisms of rosmarinic acid antiinflammatory activity.[32,33] Rosmarinic acid induces apoptosis of Jurkat and peripheral T-cells in an Lck-dependent manner, presumably through binding of Lck SH2 domain to its cognate ligands,[34] but not by inhibition of Lck kinase activity.[35] Since it has not been shown whether rosmarinic acid exhibits any influence on Fyn kinase activity, recognizing this fact could be potentially helpful in evaluation of its mechanism of action.

The three-dimensional structure of Fyn tyrosine kinase has not been reported, with the exception of solved crystal structures of Fyn SH3 or SH2 domains (or parts of these domains in complex with different substrates) which have Protein Data Bank codes 1FYN,[36] 1SHF,[37] 1NYF,[38] 1NYG,[38] 1A0N,[39] 1AVZ,[40] 1EFN,[41] 1AZG,[39] 1M27,[42] 1ZBJ,[43] 1AOT,[44] 1AOU,[44] and 1G83.[45] We briefly reported 3D model of the whole Fyn kinase molecule and characteristics of the Fyn kinase ATP-binding site domain, obtained by homology modeling.[46,47] In general, since there is a huge gap between the number of known primary protein sequences and experimentally discovered three-dimensional structures (X-ray, NMR, etc.),[48] the use of homology modeling techniques to predict 3D structures of proteins is necessary in modern drug discovery process.

Inhibition of Fyn enzyme activity with rosmarinic acid and staurosporine has been investigated using enzyme-linked immunosorbent assay (ELISA).[49,50] This type of ELISA method is based on kinase phosphorylation of immobilized substrate, which is detected using anti-tyrosine phosphate antibody. The extent of the substrate phosphorylation can be measured by absorbance, fluorescence, or fluorescence polarization.[51] Possible binding modes to the active site(s) of homology modeled Fyn kinase have been studied using the molecular docking methods and by measuring Michaelis−Menten enzyme kinetic parameters.[52] Since rosmarinic acid inhibits T-cell signaling and subsequent proliferation (presumably at the beginning of this signaling process), our aim was to examine possible inhibitory effects on Fyn kinase in order to obtain a more complete insight into antiinflammatory mechanism of action of rosmarinic acid.

Results and Discussion

Homology Modeling of Fyn Tyrosine Kinase. Fyn is proto-oncogene tyrosine-protein kinase (p59^{fyn}) classified as a phosphotransferase with the enzyme code EC 2.7.1.112.[10] The human Fyn sequence contains 537 amino acids,[53,54] composed of several functional parts that are connected together in a single protein chain (Figure 2).[55] It contains a unique N-terminal membrane anchoring segment, also called SH4 (SH = *Src*-homology) with myristylated and palmitylated N-terminal residues, SH3 and SH2 domains (which mediate interactions with proteins), a flexible linker (loop), a kinase domain (SH1), and the "final" tail at the C-terminus.

Several sequences homologous to Fyn with known 3D protein structures within the Protein Data Bank (PDB) were found (Table 1 and Figure 3)[56−59] using a BLASTP search[60] and MultAlin alignment.[61] Identity percentage and *E*-values (expectation values) are listed in Table 1. The *E*-value represents a number of different alignments with scores equivalent to or better than scores that are expected to occur in a random database search. Lower *E*-values indicate higher scores. Homologous proteins, presented in Table 1, have 62 to 77% sequence identity with Fyn tyrosine kinase. The alignment of the first 86 amino acids of Fyn was unique in comparison with the other part of the protein. We have not found any similarity for this N-terminal part of the protein between the Fyn sequence and template proteins (Figure 3). The crystal structure of the

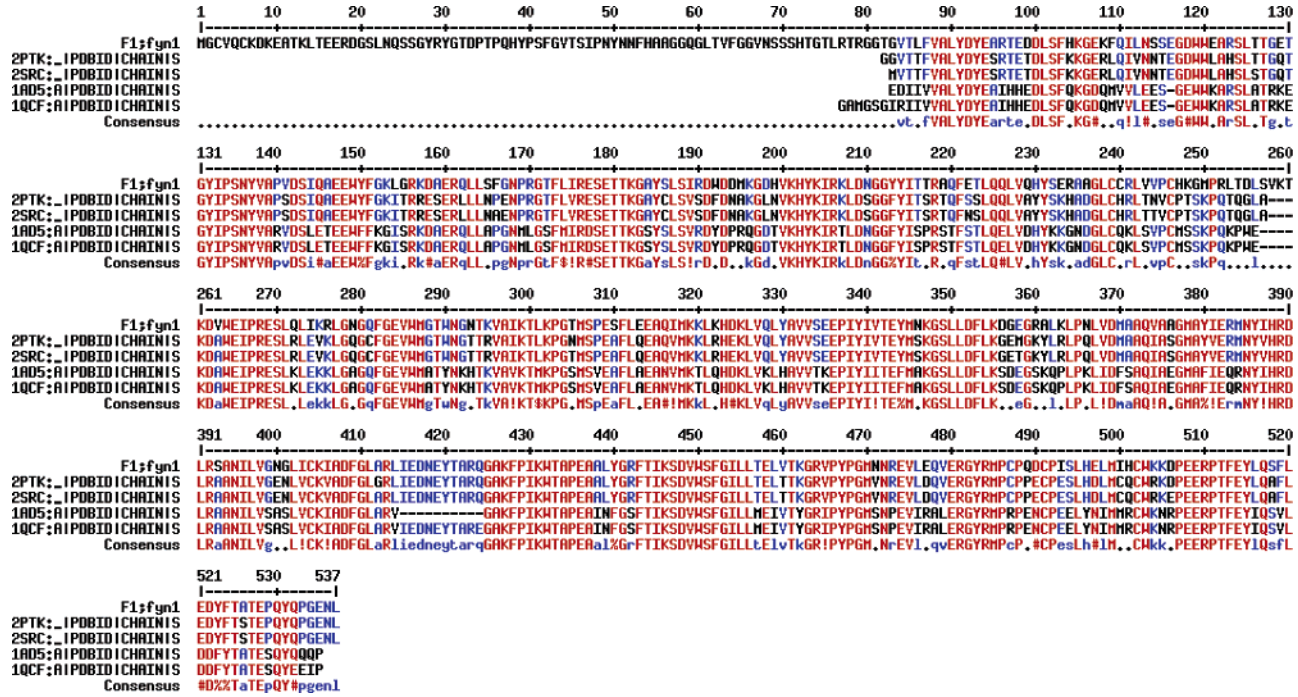

Figure 3. Primary sequence alignments of template proteins with Fyn kinase, created with MultAlin. The best alignment is shown using red letters, while structurally variable regions are shown using blue and black letters.

complex of apopain with the tetrapeptide inhibitor acetyl-Asp-Val-Ala-Asp-fluoromethyl ketone (PDB code 1CP3)[62] was found within the PDB as a suitable protein for modeling of the N-terminal part of Fyn sequence. The sequence of 1CP3 showed less than 20% homology in respect to the entire Fyn tyrosine kinase but exhibited significant homology with the unique N-terminus (amino acids 1 to 86) of Fyn (see Supporting Information, Figure S1).[63]

The resulting structure of Fyn, obtained from the modeling with Sybyl-Composer[64,65] suite of programs, was verified with the Procheck program.[66] The backbone dihedral angle distributions of all amino residues (Ramachandran Plot) were 85.7% in the most favored, 14.1% in additional allowed, and 0.2% in generously allowed regions. All other stereochemical parameters met the level of quality which would be expected from the structure of protein with a resolution of 2.0 Å.

The quality of the fold was inspected with Prosa II.[67] This software calculates the energy needed for the architecture of protein folds as a function of the amino acid sequence. Prosa II was used to calculate the energy graphs of both solved crystal structure of Src kinase (PDB-code 2SRC, the protein with the highest homology with Fyn) and the modeled structure of Fyn (Figure 4). Folding energies of proteins have generally negative values, and since these values correspond with the stability and nativity of the molecule, we can say that by modeling we obtained a reasonable structure in terms of empirical potential energy of native proteins. It can be seen from Figure 4 that in almost all parts of the sequence there is a good correlation between the modeled Fyn and the native 2SRC kinase. It is important to note that the ATP-binding site in the kinase domain, as the most important segment of the molecule, represents the most stable part of the molecule (amino acid sequence 280−420; compare Figure 2 and Figure 4). Three scores for model evaluations were examined: pair energy, surface energy, and combined pair and surface energies scores. The *Z*-score of the Fyn protein model was calculated from the above-mentioned score distributions as a function of sequence length (using regression lines and regression equation for all three score plots,

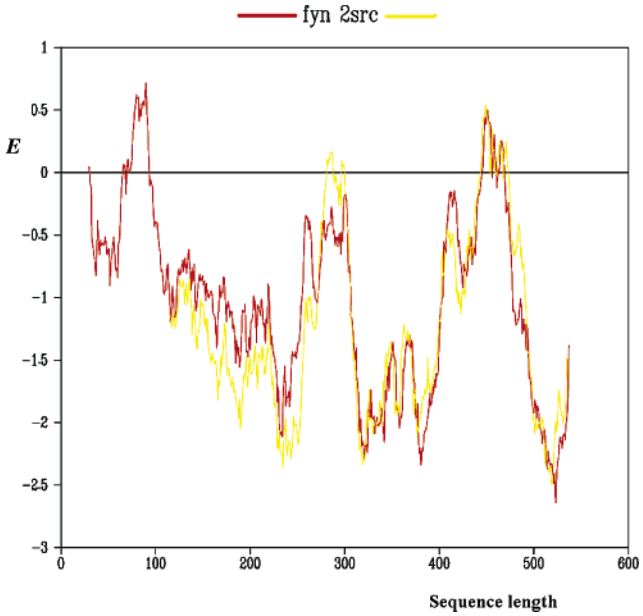

Figure 4. Energy graphs of protein folding, estimated by Prosa II software. The energy graph of the Fyn model is shown in red, and the graph of the major protein template, 2SRC, is shown in yellow.

according to the Prosa II algorithm; data not shown). The final *Z*-score of −8.4 was obtained, and this is the result of an overall energy distribution. For comparison, the Src kinase, which was used as the reference template protein, showed the same *Z*-score range. In general, the more negative the *Z*-score is, the more accurate the model is likely to be.

The secondary structure profile and its accessibility are obtained by Procheck estimations (see Supporting Information, Figure S2), while the final three-dimensional structure of Fyn, obtained by the Sybyl-Composer program, is presented in Figure 5. From the profiles of secondary and tertiary structures it can be seen that beta strands are preferred within the SH3 and SH2 domains, while within the kinase domain alpha helices structural motifs are predominant (Figure 5 and Figure S4). The ATP-

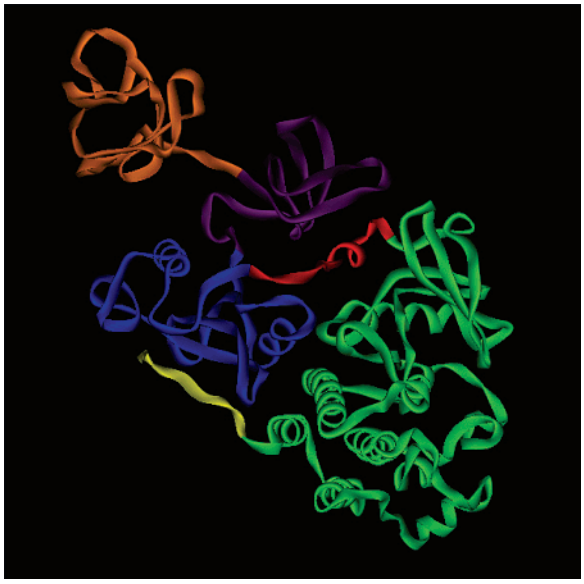

Figure 5. The three-dimensional structure of the whole molecule of Fyn tyrosine kinase, obtained by the Sybyl-Composer program. Different parts of the molecule are presented in different colors: the N-terminal part in orange, SH3 and SH2 domains in cyan and blue, respectively, flexible linker in red, kinase domain in green, and the final C-terminal tail in yellow.

binding site is located in the kinase domain opposite to the SH3 and SH2 domains. The activation segment contains 28 residues (Asp408····Glu436), which is defined in the primary sequence as the region that includes two conserved tripeptide motifs (DFG····APE) within the large lobe of the Fyn kinase domain structure. The function of the activation segment is binding of magnesium.[68] The aspartic acid residue (Asp408) is responsible for chelating magnesium and positioning of phosphates for phosphate-transfer. In this important segment with 28 residues, we observed a 100% match of the modeled Fyn structure with the structure of Src kinase (2SRC), used as the template protein. The strong homology of this segment is important since any mispositioning of magnesium-binding aspartate will have an influence on correct positioning of the ATP phosphates.[68]

Several groups reported solved crystal structures of Fyn SH3 or SH2 domains (see Introduction). The largest reported part of the Fyn kinase is the crystal structure of both SH3 and SH2 domains, comprising amino acids 81−244 (1G83.pdb).[45] This structure has been superimposed with our model of the complete Fyn structure. Folding of the domains generally match, with the exception of small deviations in some side chain conformations and not overlapping fitting in some areas (Supporting information, Figures S3 and S4). By comparing alignment of primary sequence of Fyn SH2 and SH3 domains and alignment of kinase domain with the proteins used as templates (Figure 3), it can clearly be seen that the kinase domain is evolutionarily a much more conserved region. Therefore, it can be assumed that the kinase domain part of the Fyn 3D structure is more accurately modeled than other parts of the molecule. A good match between these structures supports the general quality of our model of the complete Fyn molecule and represents a reasonable starting point for further modeling and docking investigations, as well as for ligand design and hypothesis generation.

Molecular Docking Results. To identify possible active site-(s) for docking of the ligands, the Protein Data Bank (PDB) was searched for solved crystal structures of tyrosine kinases in complex with ligands. The crystal structure of Lck complexed with staurosporine (1QPJ.pdb)[69] was spatially aligned with our model of the Fyn. Active sites of both structures were carefully analyzed, and the most important differences in the residue positions were identified. There are only a few different amino acid residues within the active site of both kinases (Lck and Fyn) such as Lys275, Asn346, and Asn400 (alignment data not shown).

Staurosporine, adenosine-5′-diphosphate, and rosmarinic acid were docked to the Fyn ATP-binding site using GOLD[70,65] and FlexX[71] docking programs. Resultant docking geometries on Fyn kinase for staurosporine and ADP were compared with the solved crystal structure of staurosporine−Lck complex (1QPJ) and AMP−Src complex (2SRC). A good match is obtained, keeping in mind that the comparison is done between similar but still different proteins (Supporting Information, Figures S5−S7). The planar part of staurosporine docked to Fyn overlaps well with this part of staurosporine in 1QPE, while some discrepancies are found for the nonplanar part of the molecule. The adenine part in ADP−Fyn complex is flipped 180° in comparison with the five-member ring moiety (sugar) of AMP−Src complex, which are oriented in the opposite directions while the phosphate groups point toward different regions of the protein surface. In general, by using FlexX, better agreement with both crystal structures was obtained. On the basis of these results and on our previous experience with kinase inhibitors (unpublished results), FlexX results are evaluated in the further discussion. Comparison with GOLD results is given in the Supporting Information (Figures S6 and S7).

Staurosporine forms three strong hydrogen bonds: NH···CO (Glu343) is 2.12 Å, CO···NH (Met345) is 1.83 Å, and NH···OH (Ser349) is 2.34 Å (Figure 6A). ADP forms three strong and one weak hydrogen bonds: N···NH (Met345) is 1.99 Å, NH···CO (Met345) 2.14 Å, PO^{-}···OH (Ser349) is 2.02 Å, and CH···CO (Glu343) is 2.62 Å (Figure 6B). The rmsd (Root-mean square deviation) values for these FlexX poses are 2.19 Å for staurosporine and 2.96 Å for ADP.

While our docking studies confirmed that ADP and staurosporine (known as ATP-competitive nonselective kinase inhibitors) bind into the ATP-binding site (binding site 1), predicted docking arrangements for rosmarinic acid allowed binding into two different but near-by binding sites (binding site 1 and binding site 2, Figures 7 and 8). Rosmarinic acid forms a network of hydrogen bonds within both sites. In site 1, the pattern is similar to both staurosporine and ADP, yet some additional H-bonds are formed. The H-bonds in site 1 (Figure 7A) are: OH···CO (Glu343) are 1.86 and 2.34 Å, OH···NH (Met345) is 2.05 Å, OH···CO (Lys347) is 1.70 Å, CO···OH (Ser349) is 1.62 Å, O^{-}···NH (Ser349) is 2.10 Å, and OH···CO (Asn346) is 2.27 Å. Seven hydrogen bonds are formed when rosmarinic acid binds into site 2 (Figure 7B): OH···NH (Asn346) is 2.10 Å, OH···CO (Tyr344) is 1.60 Å, OH···CO (Gln373) is 1.91 Å, OH···CO (Gly401) is 2.11 Å, CO···NH (Arg252) are 1.93, 1.91, 2.11, and 2.02 Å. The rmsd between FlexX and GOLD poses for rosmarinic acid docked into the site 1 is 9.12 Å. Such a big difference is due to the flipped orientation of the rosmarinic acid obtained by GOLD (Supporting Information, Figure S6B). The rmsd for rosmarinic acid docked into the site 2 is 2.47 Å.

From our docking experiments, rosmarinic acid binding could occur on Fyn kinase domain ATP-binding site, or on the opposite site from the kinase ATP-binding site (Figure 8). This "binding site 2" is in the kinase domain but oriented toward the linker which connects SH2 and kinase domains. Peptide substrate binding regions (SH2 and SH3 domains) of Fyn are

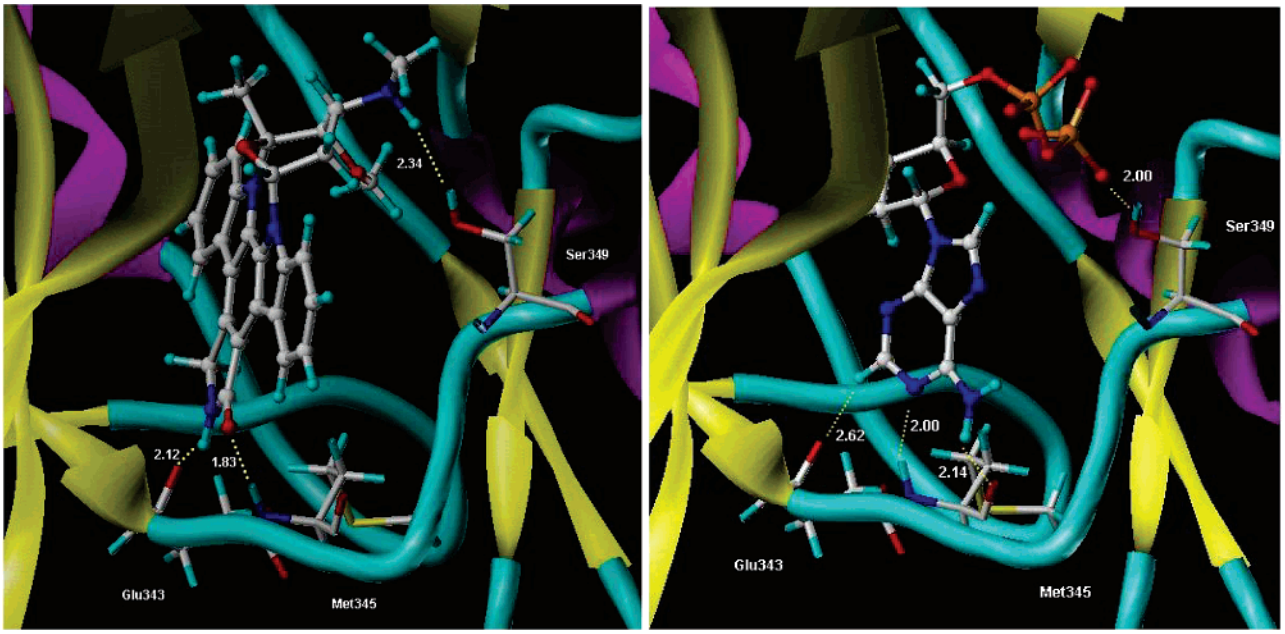

Figure 6. The structure of the Fyn kinase domain ATP-binding site with (A) staurosporine and (B) adenosine-5′-diphosphate docked with FlexX into the binding site. Hydrogen bonds are presented as dotted lines. Distances are given in Å.

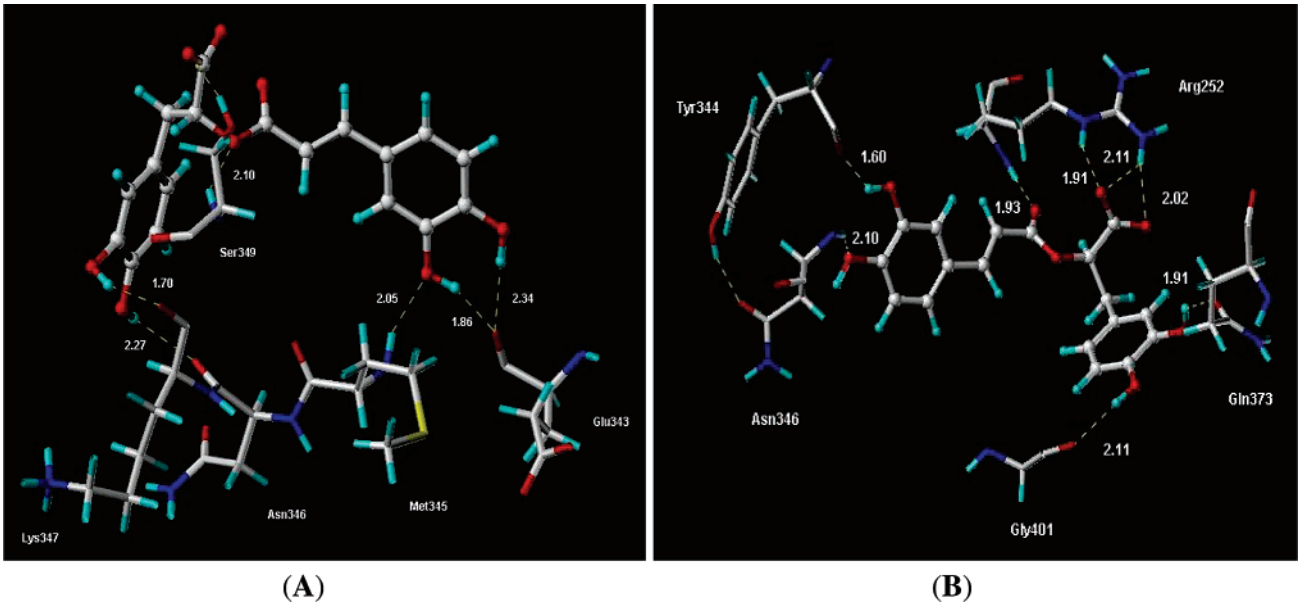

Figure 7. Rosmarinic acid docked to (A) binding site 1 and (B) binding site 2. Hydrogen bonds are presented as dotted lines. Distances are given in angstroms.

still far from the kinase domain ATP-binding site and "binding site 2". But, interesting and important interaction with Arg252 is observed in the case of rosmarinic acid binding to site 2. Arg252 is a part of the segment, which links the SH2 domain with the kinase domain (SH2-kinase linker), and forms a short polyproline type II helix. This SH2-kinase linker in Hck (one of the template proteins) contains a PXXP motif, the minimum consensus sequence for binding to SH3 domains, but the linker in Fyn kinase (as well as in the Src template protein) contains only one proline. Also, high-affinity binding of SH3 domains to proline-rich sequences generally requires an arginine or lysine on either side of the PXXP motif,[72] which are absent in the Fyn linker but present in Hck linker. In the crystal structure of Src kinase, a new intramolecular interaction between SH3 domain and SH2-kinase linker is observed.[56] Therefore, interaction with a residue from this linker could have some influence on protein−protein interactions usually occurring via SH2 or/and SH3 domains. Also, an "induced fit" effect on ATP-binding site is possible, since binding site 2 is located on the backside of ATP-binding site (Figure 8). Both FlexX and GOLD slightly prefer binding of rosmarinic acid into the binding site 2 (Table 2), although the difference in scoring values is not statistically significant. Is a possible scenario that rosmarinic acid binds into both sites, with somewhat different affinity for the binding site 2? An answer to this question was found in enzyme kinetics experiments, but the real proof can only be obtained by performing cocrystallization experiments with Fyn kinase and rosmarinic acid as the ligand.

***In Vitro* Kinase Inhibition and Enzyme Kinetics.** Inhibition of Fyn kinase activity by rosmarinic acid and staurosporine was

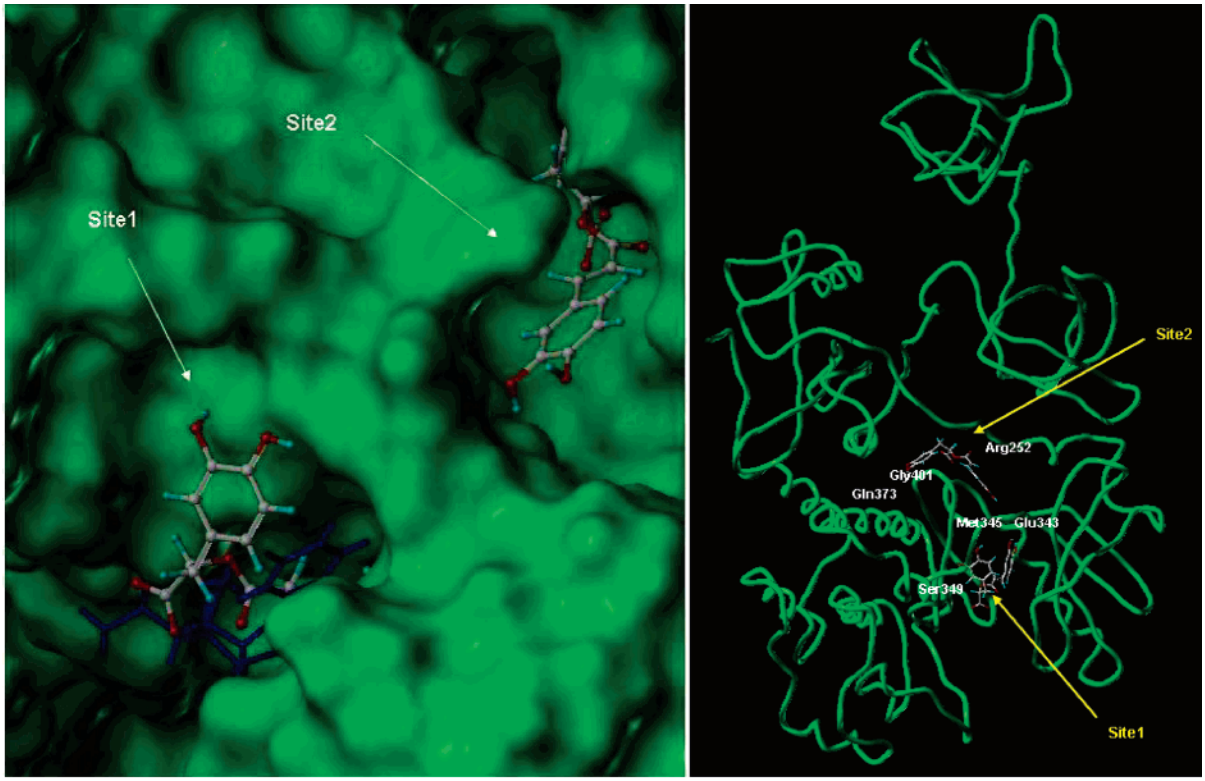

Figure 8. Fyn kinase with rosmarinic acid docked to the two binding sites. **(**A**)** Molecular surface representation of the binding region with sites 1 and 2. Rosmarinic acid is colored by atom types, and staurosporine is shown in blue. **(**B**)** Whole Fyn kinase model with important amino acids marked in white.

Table 2. FlexX Scoring Values for Predicted Binding Modes of Rosmarinic Acid, Staurosporine, and Adenosine-5′-diphosphate (GOLD scores are given in parentheses)

	position	
compound	binding site 1	binding site 2
rosmarinic acid	−22.2 (52.4)	−24.2 (59.3)
adenosine-5-diphosphate	−21.6 (63.9)	−
staurosporine	−30.3 (63.6)	−

Table 3. Inhibition of Human Fyn Kinase Activity (IC_{50} values) by Rosmarinic Acid and Staurosporine, in the Presence of Different ATP Concentrations[a]

		IC_{50} (Fyn)/μmol/L		
compound	kinase reaction time, min	1 μmol/L ATP	10 μmol/L ATP	100 μmol/L ATP
rosmarinic acid	20	1.3	3.6	17
	1	36	74	63
staurosporine	20	0.015	0.083	0.51
	1	0.005	0.036	0.270

[a] Poly Glu:Tyr (4:1) in constant concentration was used as substrate, in all experiments. Kinase reaction times were 1 and 20 min. Inhibitors were tested using eight different concentrations of rosmarinic acid, in 10-fold dilution from 3 mmol/L to 0.3 nmol/L.

tested by ELISA method. According to our results, rosmarinic acid inhibits Fyn tyrosine kinase in low micromolar concentrations (IC_{50} = 1.3 μmol/L) in a dose-dependent manner. Staurosporine, a standard nonselective kinase inhibitor, inhibits Fyn kinase in nanomolar concentrations (IC_{50} = 15 nmol/L) (Table 3).

According to the rosmarinic acid inhibition results, and since inhibition of Fyn kinase is a new biological indication for rosmarinic acid, we performed enzyme kinetics experiments in order to evaluate the mechanism of Fyn kinase inhibition. ATP-competitive as well as other types of inhibition should follow Michaelis−Menten kinetics in its linear range.[52] The linearity range of Michaelis−Menten kinetics for Fyn kinase with ATP as substrate was inspected, and linearity was observed up to 5 min of kinase reaction (data not shown). The inhibitory effect of rosmarinic acid at two different concentrations, measured after 30 and 60 s of kinase reaction times and using seven different ATP concentrations, obeyed Michaelis−Menten kinetics (Figure 9). The V_{max}, K_m, and K_i parameters were calculated for Fyn with ATP and without inhibitor, or with ATP and using two concentrations of rosmarinic acid as inhibitor. From Figure 9 and Table 4, it can be seen that rosmarinic acid caused apparent decrease of V_{max} value and apparent increase of K_m value, with excellent fit of the model to the data (Table 4). Kinetics data implicate that rosmarinic acid inhibits Fyn kinase in a linear-mixed type of inhibition. In this type of reversible inhibition, a compound can interact both with the free enzyme and with the enzyme−substrate complex at a site other than the active site, as can be seen from the scheme in Figure 10.

By changing the concentrations of ATP in the ELISA kinase assay, we examined the inhibitory mode of rosmarinic acid (Table 3). By not considering the kinetics data, from results obtained after 20 min of kinase reaction time, it could be concluded that rosmarinic acid inhibits Fyn in an ATP-dependent manner (Table 3, i.e., by binding into the ATP-binding pocket or near to that pocket), since the decrease in rosmarinic acid inhibitory activity corresponds to increased ATP concentrations. But, from enzyme kinetics data (Table 4), when the kinase reaction was performed in the linear range (1 min, Table 3), the competitivity of rosmarinic acid with ATP was not observed. Also, in this unsaturated part of the Michaelis−Menten curve, the inhibitory potency of rosmarinic acid was decreased (Table 3). The inhibitory profile of rosmarinic acid was compared with

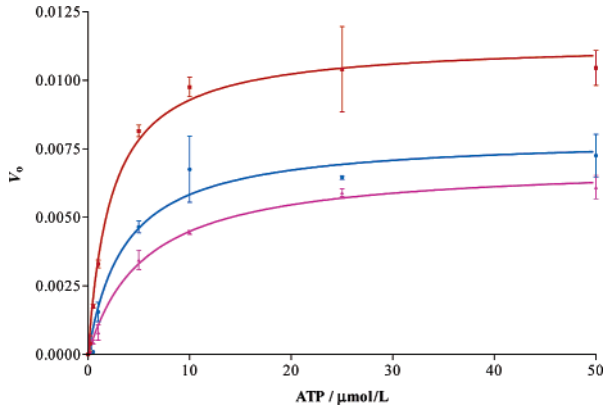

Figure 9. Fyn kinase kinetics experiments with different concentrations of ATP as a substrate (0.2, 0.5, 1, 5, 10, 25, and 50 μmol/L) and by addition of two different concentrations of rosmarinic acid (red line = Fyn-ATP curve without inhibitor, blue line = 10 μmol/L rosmarinic acid, purple line = 30 μmol/L rosmarinic acid). Two experiments were performed, and the mean and corresponding standard deviations indicated as bars were calculated and presented. Nonlinear regression curve has been used (curve fit), by the equation $Y = V_{max}*X/(K_m + X)$, which describes the binding of a ligand to a receptor that follows the law of mass action. V_{max} is the maximal binding, and K_m is the concentration of ligand required to reach half-maximal binding.

staurosporine, a known ATP-competitive nonselective tyrosine kinase inhibitor.[73] It can be seen in Table 3, that under the same reaction conditions, staurosporine acts as an ATP-competitive inhibitor after 20 min, as well as after 1 min, of kinase reaction. This was not observed in the rosmarinic acid inhibitory profile.

The above-mentioned findings are in a good correlation with the docking results where an additional binding site near to the ATP-binding site was proposed. Although statistically not significant, a slightly higher binding affinity of rosmarinic acid binding to site 2, (Figures 7, 8 and Table 2) was observed. In the case that rosmarinic acid preferably binds to the binding site 2, this could explain the obtained linear-mixed inhibition profile. On the other hand, occupation of the binding site 2 with rosmarinic acid could still have some influence on the ATP-binding site, since this site is located at the back side of the rosmarinic acid-binding site (see Figures 7 and 8). Conformational changes after binding of rosmarinic acid into the site 2 could cause an inhibitory effect by decreasing the rate of ATP binding into its active site. When the kinase reaction is performed in the linear range, it can be seen that rosmarinic acid acts in a manner which is noncompetitive with ATP. However, after 20 min of kinase reaction time (outside the linearity range), an "induced fit" influence on the ATP-binding site could occur, due to possible conformational changes near to the ATP-binding pocket.

Rosmarinic acid was previously reported as an inhibitor of TCR-signaling and subsequent T-cell proliferation, presumably via inhibition of the Lck SH2 domain by binding to the peptide that contains consensus binding sequence (pYEEI).[34] It inhibited TCR-induced Ca^{2+} mobilization and IL-2 promoter activation, but not phorbol 12-myristate 13-acetate (PMA)/ionomycin-induced IL-2 promoter activation, indicating that the point of inhibition of rosmarinic acid is near to the membrane, proximal to TCR signaling site.[32] TCR-inhibition is limited to TCR-induced but not to PMA/ionomycin-induced IL-2 promoter activation. Therefore, it was concluded that rosmarinic acid works upstream of protein kinase C and Ca^{2+} flux, by suppressing NF-AT promoter activation (but not AP-1) through inhibition of the membrane-proximal events, specifically, the tyrosine phosphorylation of PLC-γ1 and Itk.[33] Since both Fyn and Lck are involved in the initial tyrosine phosphorylation of T-cell receptor, we are proposing Fyn kinase activity inhibition as an additional mechanism by which rosmarinic acid performs its anti-inflammatory action. Furthermore, in regard to Lck−Fyn correlation, experiments with $Fyn^{-/-}$ and $Lck^{-/-}$ mice were performed and it was shown that in $Fyn^{-/-}$ mice thymocite growth was normal, while that was not the case in the $Lck^{-/-}$ mice. In the absence of Lck ($Lck^{-/-}$ mice), IL-2 production was completely inhibited, while in the absence of Fyn ($Fyn^{-/-}$), the production of this T-cell growth factor was just moderately inhibited.[74,75] These results could define Fyn kinase as a suitable target for the treatment of some diseases, such as autoimmunity or cancer.

Conclusions

Because of their role in regulation of physiological mechanisms, including cell proliferation, differentiation, and metabolism, tyrosine kinases represent one of the most important targets in pharmaceutical research.[1] Interruption of the signaling pathways with some specific inhibitors could prevent cell activation, differentiation, and proliferation, plus could be useful in treating diseases such as cancer, allergy, autoimmunity,[76] or cardiovascular diseases, such as hypertrophy, ischemia, angiogenesis, and atherogenesis.[77] Recent papers suggest also that some *Src*-family kinases (including Fyn) could be suitable targets for therapeutic modulation in Alzheimer's disease, and for the development of novel disease-modifying antiinflammatory therapy.[78] Newest early Phase I and II studies in airway inflammatory diseases suggest that inhibitors of p38, MAP kinase, and IKK2 could be used as novel therapies in the treatment of asthma, COPD, and cystic fibrosis.[79] Within past few years, more than 40 drugs or clinical candidates, which were discovered using structure-based approach, came to the market or are in final step of the clinical research.[80,81] The solved three-dimensional structure of Fyn tyrosine kinase could help in using structure-based drug design as a method for designing novel specific Fyn kinase inhibitors. Therefore, an important task of this study was a good prediction of the 3D structure of Fyn kinase domain and its active site(s). The *Z*-score value, obtained from energy plots of modeled kinase,[67] indicate that our Fyn model represents a structurally reasonable protein structure, which can be a good starting point for further modeling and docking investigations.

In the presented study we identified precisely the active site of Fyn kinase. Also, we were able to use molecular modeling methods to dock ligands into the active site. The agreement between our 3D structure of Fyn and crystal structure of Lck kinase, as well as experimentally determinated structures of SH2 and SH3 domains of Fyn, highly support the fact that the quality of our Fyn model is adequate for further investigations like docking and *in silico* ligand design. By using ELISA experiments, rosmarinic acid as a low micromolar inhibitor of Fyn tyrosine kinase has been demonstrated. Staurosporine, a standard ATP-competitive and nonselective kinase inhibitor, in our case proved to inhibit Fyn kinase in nanomolar concentrations. On the basis of the results of the kinetic measurements, we are proposing a linear-mixed mechanism of Fyn kinase activity inhibition by rosmarinic acid. These results indicate that rosmarinic acid inhibits Fyn by interacting both with the free enzyme and with the enzyme−substrate complex at a site other than the ATP-binding site. Docking studies performed on our homology model of Fyn kinase, together with the results obtained from kinetic studies, suggest the existence of another

Table 4. Fyn Michaelis−Menten Nonlinear Regression Curve Parameters

complex	V_{max}	V_{max} Std. error	K_m/μmol/L	K_m Std. error	K_i/μmol/L	r^2 (goodness of fit)
Fyn−ATP	0.0114	0.00034	2.292	0.31	−	0.984
Fyn−ATP with 10 μmol/L of rosmarinic acid	0.00793	0.00046	3.616	0.85	7.5	0.959
Fyn−ATP with 30 μmol/L of rosmarinic acid	0.00696	0.00020	5.523	0.58	10.2	0.992

[a] Equation used for curve fit is $Y = V_{max}*X/(K_m + X)$, which describes the binding of a ligand to a receptor that follows the law of mass action. V_{max} is the maximal binding, K_m is the concentration of ligand required to reach half-maximal binding, and K_i is inhibition constant. Best-fit values (r^2), std error, 95% confidence intervals, and goodness of fit were calculated for each curve. K_i was calculated by comparison of V_{max} and K_m values for curves without and with inhibitors. In the case of linear-mixed inhibition, $V_{max}* = V_{max}/\beta$ and $K_m* = (\alpha/\beta)K_m$, where $\alpha = 1 + [I]/K_i$. $V_{max}*$ and K_m* correspond, respectively, to the apparent enzyme maximum velocity and apparent enzyme−substrate dissociation constant in the presence of an inhibitor.

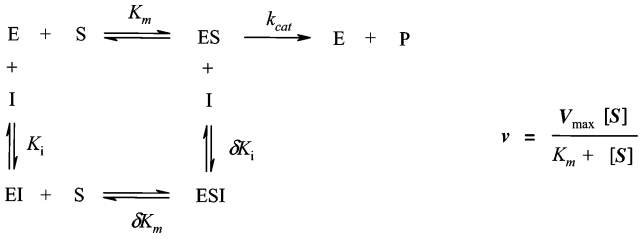

Figure 10. Linear-mixed inhibition and the basic Michaelis−Menten equation.[52] V_{max} corresponds to the apparent enzyme maximum velocity, K_m represents apparent enzyme−substrate dissociation constant, E is enzyme, S is substrate, ES is enzyme−substrate complex, EI is enzyme−inhibitor complex, ESI is enzyme−substrate−inhibitor complex, and P is product.

binding pocket on the opposite site to the ATP-binding pocket. Binding of rosmarinic acid to this new binding site could cause some competition with ATP because of the proximity of the substrate-binding site. Also, almost the same residues are occupied by forming hydrogen bonds with both ATP in site 1 and rosmarinic acid in site 2. Rosmarinic acid has been reported as an inhibitor of TCR-signaling and subsequent T-cell proliferation, presumably *via* inhibition of Lck SH2 domain and its peptide substrate interaction.[32] Since we recognized an interesting and important interaction of rosmarinic acid bound to site 2, with the segment linking the SH2 domain with the kinase domain, we cannot exclude some influence of this inhibitor on Fyn protein−protein interactions. According to our findings, we are proposing direct inhibition of Fyn kinase activity by rosmarinic acid as an important fact in rosmarinic acid antiinflammatory mechanism(s) of action.

Experimental Section

Homology Modeling. Human Fyn primary sequence,[53] and sequences of other different protein species, were retrieved either from literature or available macromolecular data bases.[34,54] Sequences homologous to Fyn were obtained from the Protein Data Bank (PDB) by using a BLASTP search[60] and compared by using MultAlin alignment.[61] For homology modeling, the Composer set of programs within Sybyl 6.7 (TRIPOS)[64,65] was used. On the basis of the alignment, structurally conserved regions (SCRs) were automatically created and structurally variable regions (SVRs) were defined. Some SVRs were modeled afterward using the Loop Search option in Sybyl. The obtained tertiary structure was refined by minimization with the AMBER force field.[82] The active sites of the enzyme with docked ligands obtained from GOLD dockings were optimized using the TRIPOS force field[83] to allow induced fit. The stereochemical quality of the protein structure was checked with Procheck.[66] Prosa II[67] was used to check the native folding of the modeled structure by calculation of the *Z*-score, which is the score of pair and surface energies based on mean force potentials of the model. The corresponding energy graphs were compared with the structure of template protein 2SRC (PDB code).[56]

Molecular Docking. Two different approaches have been used for molecular docking studies: the GOLD program (Ver. 2.0, CCSD)[70,65] and the FlexX[71] program. The three-dimensional structures of rosmarinic acid, ADP, and staurosporine were constructed using the molecular modeling program package Sybyl,[64] followed by energy optimizations with the TRIPOS force field.[83] Ligands were docked to Fyn using standard settings for FlexX and default parameters for GOLD. The binding site was defined from the residues within 10 and 15 Å from staurosporine, used as a reference ligand in accordance with the template protein 1QPJ (PDB code).[69] DrugScore and GOLDScore scoring functions were used during docking process and as fitness functions.

***In Vitro* Kinase Inhibition and Enzyme Kinetics.** Fyn protein kinase was expressed in *Sf9* (*Spodoptera frugiperda* ovary cell) baculovirus expression system and thereafter purified using chromatography methods. Purification and characterization were performed in GSK Research Centre Zagreb, according to literature protocols.[84−86]

Staurosporine (S-4400), *O*-phenylenediamine substrate (P-8287), HEPES (H-3375), $MgCl_2$ (M-8266), BSA (bovine serum albumin, A-2153), ATP (adenosine 5′-triphosphate disodium salt, A-6419), adenosine-5′-diphosphate sodium salt (A-2754), and kinase substrate (random polypeptide copolymer Poly Glu:Tyr (4:1), P-0275) were obtained from Sigma. Peroxidase-labeled anti-phosphotyrosine antibody PY20 (mouse) was obtained from Calbiochem (525320). Rosmarinic acid (3,4-dihydroxycinnamic acid, (*R*)-1-carboxy-2-(3,4-dihydroxyphenyl)ethyl ester) was obtained from Alexis (ALX-270−253). Tween 20 (polyoxyethylene sorbiton monolaureate, 17-1316-01) was obtained from Pharmacia. $MnCl_2$ (8.05930.0100) and H_2O_2 (1.07298.1000) were obtained from Merck. DTT (dithiothreitol, 161-0611) was obtained from Bio-Rad. Measurements were performed by a Multiscan Ascent spectrophotometer (ThermoLabSystem).

In vitro inhibition of Fyn kinase by rosmarinic acid and staurosporine was monitored according to a previously published ELISA method.[87,88] Phosphorylation of the substrate was monitored by an immunochemical reaction, where phosphorylated substrate residues were detected by a specific immunocomplex and absorbance was measured at 490 nm. ELISA experiments were conducted in 96-well Dynex Immulon 2 HB microtitar plates (flat bottom, transparent). Peptide substrate in constant concentration of 10 μg/well was coated to the plate. After washing, buffer solution with ATP was added to each well. Compounds were added into wells in final concentrations from 10^{-3} mol/L to 10^{-11} mol/L. Fyn kinase in a concentration of 100 ng/well was added, and the kinase reaction lasted 1 min in one type and 20 min in the other type of experiment. After washing, blocking of the wells with 1% BSA in TBS was performed. Peroxidase-labeled anti-phosphotyrosine antibody was then added and incubated for 40 min. After washing, peroxidase substrate[89] was added and reaction was stopped after 20 min with 5 M H_2SO_4. Absorbance was measured at 490 nm.

Preliminary ATP-competitivity measurements were assayed in the presence of different ATP concentrations (1, 10, and 100 μmol/L), using a constant concentration of the peptide substrate, after 1 or 20 min of kinase reaction. The IC_{50} value was calculated by using GraphPad Prism software, v. 3.02. The IC_{50} point of inflection is defined as concentration of compound which inhibits 50% of enzyme activity (where inserted parameters simulated sigmoidal dose−response theoretical curve).

The same ELISA experimental procedure was used in enzyme kinetics experiments when the linearity range of Michaelis−Menten kinetics for Fyn kinase with ATP as substrate was investigated. The inhibitory effect of compounds (two concentrations; 10 and

30 μmol/L) was measured after 30 and 60 s of kinase reactions using seven different concentrations of ATP (0.2, 0.5, 1, 5, 10, 25, and 50 μmol/L). By using GraphPad Prism software, Michaelis−Menten kinetic curves, together with V_{max}, K_m, and K_i parameters were also calculated. A nonlinear regression (curve fit) curve has been created by using the equation $Y = V_{max}*X/(K_m + X)$, which describes the binding of a ligand to a receptor, that follows the law of mass action. V_{max} is the maximal binding, and K_m is the concentration of ligand required to reach half-maximal binding. Best-fit values, std error, 95% confidence intervals, and goodness of fit were calculated for each curve. K_i was calculated by comparison of V_{max} and K_m values for curves with and without inhibitors. In the case of linear-mixed inhibition, $V_{max}* = V_{max}/\beta$ and $K_m* = (\alpha/\beta)K_m$, where $\alpha = 1 + [I]/K_i$. $V_{max}*$ and K_m* correspond, respectively, to the apparent enzyme maximum velocity and apparent enzyme−substrate dissociation constant in the presence of an inhibitor.

Note Added in Manuscript Revision

After submission of this article, we recognized a paper published on this topic [Kinoshita, T. *et al. Biochm. Biophys. Res. Commun.* **2006**, *346*, 840−844, published in PDB on July 7, 2006], where the authors presented a low-resolution (2.8 Å) structure of the Fyn kinase domain with staurosporine in the active site. By comparing our modeling and docking work with the results of Kinoshita *et al.*, excellent agreement with our findings was observed, both in the architecture of the kinase domain Fyn 3-D structure (Supporting Information, Figure S4) as well as in the staurosporine orientation in the Fyn active site.

Acknowledgment. We thank Prof. Ludger Wessjohann for his hospitality in Leibniz-Institute of Plant Biochemistry in Halle (Saale) where the homology modeling part of this work has been done, and also for reading of this paper, as well as Dr. Lars Bräuer for his great help and suggestions. Many thanks to Dr. William Andrew Irwin for the critical assessment and grammar corrections of the manuscript. The authors are grateful to all persons from GlaxoSmithKline Research Centre Zagreb, which participated in Fyn kinase expression, isolation, and characterization. Also, we appreciate the great help we received from our technicians Ana Cvetković, Klara Markušić, Andrej Tkalčević and Željka Tolić.

Supporting Information Available: Additional figures with Fyn kinase 3D structure characterization and comparison with crystal structures from the literature. Also, comparisons of docking poses for rosmarinic acid, staurosporine, and ADP/AMP obtained by FlexX and GOLD docking programs. This material is available free of charge via the Internet at http://pubs.acs.org.

References

(1) Mellado, M.; Rodriguez-Frade, J. M.; Manes, S.; Martinez, A. C. Chemokine signaling and functional responses: the role of receptor dimerization and TK pathway activation. *Annu. Rev. Immunol.* **2001**, *19*, 397−421.
(2) Hanks, S. K.; Hunter, T. Protein kinases 6. The eukaryotic protein kinase superfamily: kinase (catalytic) domain structure and classification. *FASEB J.* **1995**, *9*, 576−596.
(3) Johnson, L. N.; Lewis, R. J. Structural basis for control by phosphorylation. *Chem. Rev.* **2001**, *101*, 2209−2242.
(4) Milanesi, L.; Petrillo, M.; Sepe, L.; Boccia, A.; D'Agostino, N.; Passamano, M.; Di Nardo, S.; Tasco, G.; Casadio, R.; Paolella, G. Systematic analysis of human kinase genes: a large number of genes and alternative splicing events result in functional and structural diversity. *BMC Bioinf.* **2005**, *6* (4), S20.
(5) Krupa, A.; Srinivasan, N. The repertoire of protein kinases encoded in the draft version of the human genome: atypical variations and uncommon domain combinations. *Genome Biol.* **2002**, *3* (12), 0066/1−14.
(6) Saito, H. Histidine phosphorylation and two-component signaling in eukaryotic cells. *Chem. Rev.* **2001**, *101*, 2497−2510.
(7) Hubbard, S. R.; Till, J. H. Protein tyrosine kinase structure and function. *Annu. Rev. Biochem.* **2000**, *69*, 373−398.
(8) Neel, B. G.; Tonks, N. K. Protein tyrosine phosphatases in signal transduction. *Curr. Opin. Cell. Biol.* **1997**, *9*, 193−204.
(9) Robinson, D. R.; Wu, Y-M.; Lin, S. F. The protein tyrosine kinase family of the human genome. *Oncogene* **2000**, *19*, 5548−5557.
(10) Bairoch, A. The ENZYME data bank. *Nucleic Acids Res.* **1993**, *21* (13), 3155−3156.
(11) Cooke, M. P.; Abraham, K. M.; Forbush, K. A.; Perlmutter, R. M. Regulation of T cell receptor signaling by a src family protein-tyrosine kinase (p59fyn). *Cell* **1991**, *65* (2), 281−91.
(12) Davidson, D.; Chow, L. M.; Fournel, M.; Veillette, A. Differential regulation of T cell antigen responsiveness by isoforms of the src-related tyrosine protein kinase p59fyn. *J. Exp. Med.* **1992**, *175* (6), 1483−1492.
(13) Wange, R. L.; Samelson, L. E. Complex complexes: signaling at the TCR. *Immunity* **1996**, *5*, 197−205.
(14) Utting, O.; The, S. J.; The, H. S. T cells expressing receptors of different affinity for antigen ligands reveal a unique role for p59fyn in T cell development and optimal stimulation of T cells by antigen. *J. Immunol.* **1998**, *160* (11), 5410−5419.
(15) Da Silva, A. J.; Janssen, O.; Rudd, C. E. T cell receptor zeta/CD3−p59fyn(T)-associated p120/130 binds to the SH2 domain of p59fyn-(T). *J. Exp. Med.* **1993**, *178* (6), 2107−2113.
(16) Timson Gauen, L. K.; Linder, M. E.; Shaw, A. S. Multiple Features of the p59^{fyn} src Homology 4 Domain Define a Motif for Immune-Receptor Tyrosine-based Activation Motif (ITAM) Binding and for Plasma Membrane Localization. *J. Cell Biol.* **1996**, *133* (5), 1007−1015.
(17) Samelson, L. E.; Phillips, A. F.; Luong, E. T.; Klausner, R. D. Association of the fyn protein-tyrosine kinase with the T-cell antigen receptor. *Proc. Natl. Acad. Sci. U.S.A.* **1990**, *87*, 4358−4362.
(18) Zhang, W.; Sloan-Lancaster, J.; Kitchen, J.; Trible, J.; Samelson, L. E. LAT: the ZAP-70 tyrosine kinase substrate that links T cell receptor to cellular activation. *Cell* **1998**, *92*, 83−92.
(19) Wardenburg, J. B.; Fu, C.; Jackman, J. K.; Flotow, H.; Wilkinson, S. E.; Williams, D. H.; Johnson, R.; Kong, G.; Chan, A. C.; Findell, P. R. Phosphorylation of SLP-76 by the ZAP-70 protein-tyrosine kinase is required for T-cell receptor function. *J. Biol. Chem.* **1996**, *271*, 19641−19644.
(20) Samelson, L. E.; Patel, M. D.; Weissman, A. M.; Harford, J. B.; Klausner, R. D. Antigen activation of murine T cells induces tyrosine phosphorylation of a polypeptide associated with the T cell antigen receptor. *Cell* **1986**, *46*, 1083−1090.
(21) Filipp, D.; Leung, B. L.; Zhang, J.; Veillette, A.; Julius, M. Enrichment of lck in lipid rafts regulates colocalized fyn activation and the initiation of proximal signals through TCR alpha beta. *J. Immunol.* **2004**, *172* (7), 4266−74.
(22) Liang, X.; Lu, Y.; Wilkes, M.; Neubert, T. A.; Resh, M. D. The N-terminal SH4 Region of the Src Family Kinase Fyn Is Modified by Methylation and Heterogeneous Fatty Acylation. *J. Biol. Chem.* **2004**, *279* (48), 8133−8139.
(23) Van't Hof, W.; Resh, M. D. Rapid Plasma Membrane Anchoring of Newly Synthesized p59fyn: Selective Requirement for NH_2-Terminal Myristoylation and Palmitoylation at Cysteine-3. *J. Cell Biol.* **1997**, *136* (5), 1023−1035.
(24) Alland, L.; Peseckis, S. M.; Atherton, R. E.; Berthiaume, L.; Resh, M. D. Dual Myristylation and Palmitylation of Src Family Member p59^{fyn} Affects Subcellular Localization. *J. Biol. Chem.* **1994**, *269* (24), 16701−16705.
(25) Horejsi, V. The roles of membrane microdomains (rafts) in T cell activation. *Immunol. Rev.* **2003**, *191*, 148−64.
(26) Filipp, D.; Zhang, J.; Leung, B. L.; Shaw, A.; Levin, S. D.; Veillette, A.; Julius, M. Regulation of Fyn through translocation of activated Lck into lipid rafts. *J. Exp. Med.* **2003**, *197* (9), 1221−7.
(27) Prade, L.; Engh, R. A.; Girod, A.; Kinzel, V.; Huber, R.; Bossemeyer, D. Staurosporine-induced conformational changes of cAMP-dependent protein kinase catalytic subunit explain inhibitory potential. *Structure* **1997**, *5* (12), 1627−1637.
(28) Toledo, L. M.; Lydon, N. B. Structures of staurosporine bound to CDK2 and cAPK-new tools for structure-based design of protein kinase inhibitors. *Structure* **1997**, *5* (12), 1551−1556.
(29) Al-Sereiti, M. R.; Abu-Amer, K. M.; Sen, P. Pharmacology of rosemary (Rosmarinus officinalis Linn.) and its therapeutic potentials. *Indian J. Exp. Biol.* **1999**, *37* (2), 124−30.
(30) Iuvone, T.; De Filippis, D.; Esposito, G.; D'Amico, A.; Izzo, A. A. The Spice Sage and Its Active Ingredient Rosmarinic Acid Protect PC12 Cells from Amyloid-beta Peptide-Induced Neurotoxicity. *J. Pharmacol. Exp. Ther.* **2006**, *317* (3), 1143−1149.
(31) Lee, J.; Jung, E.; Kim, Y.; Lee, J.; Park, J.; Hong, S.; Hyun, C. G.; Park, D.; Kim, Y. S. Rosmarinic acid as a downstream inhibitor of IKK-beta in TNF-alpha-induced upregulation of CCL11 and CCR3. *Br. J. Pharmacol.* **2006**, *148* (3), 366−375.

(32) Won, J.; Hur, Y. G.; Hur, E. M.; Park, S. H.; Kang, M. A.; Choi, Y.; Park, C.; Lee, K. H.; Yun, Y. Rosmarinic acid inhibits TCR-induced T cell activation and proliferation in an Lck-dependent manner. *Eur. J. Immunol.* **2003**, *33*, 870−879.
(33) Kang, M. A.; Yun, S. Y.; Won, J. Rosmarinic acid inhibits Ca^{2+}-dependent pathways of T-cell antigen receptor-mediated signaling by inhibiting the PLC-γ1 and Itk activity. *Blood* **2003**, *101* (9), 3534−3542.
(34) Ahn, S. C.; Oh, W. K.; Kim, B. Y.; Kang, D. O.; Kim, M. S.; Heo, G. Y.; Ahn, J. S. Inhibitory effects of rosmarinic acid on Lck SH2 domain binding to a synthetic phosphopeptide. *Planta Med.* **2003**, *69* (7), 642−646.
(35) Hur, Y-G.; Yun, Y.; Won, J. Rosmarinic Acid Induces $p56^{lck}$-Dependent Apoptosis in Jurkat and Peripheral T Cells via Mitochondrial Pathway Independent from Fas/Fas Ligand Interaction. *J. Immunol.* **2004**, *172*, 79−87.
(36) Musacchio, A.; Saraste, M.; Wilmanns, M. High-resolution crystal structures of tyrosine kinase SH3 domains complexed with proline-rich peptides. *Nat. Struct. Biol.* **1994**, *1*, 546−551.
(37) Noble, M. E.; Musacchio, A.; Saraste, M.; Courtneidge, S. A.; Wierenga, R. K. Crystal structure of the SH3 domain in human Fyn; comparison of the three-dimensional structures of SH3 domains in tyrosine kinases and spectrin. *EMBO J.* **1993**, *12*, 2617−2624.
(38) Morton, C. J.; Pugh, D. J.; Brown, E. L.; Kahmann, J. D.; Renzoni, D. A.; Campbell, I. D. Solution structure and peptide binding of the SH3 domain from human Fyn. *Structure* **1996**, *4*, 705−714.
(39) Renzoni, D. A.; Pugh, D. J.; Siligardi, G.; Das, P.; Morton, C. J.; Rossi, C.; Waterfield, M. D.; Campbell, I. D.; Ladbury, J. E. Structural and thermodynamic characterization of the interaction of the SH3 domain from Fyn with the proline-rich binding site on the p85 subunit of PI3-kinase. *Biochemistry* **1996**, *35*, 15646−15653.
(40) Arold, S.; Franken, P.; Strub, M. P.; Hoh, F.; Benichou, S.; Benarous, R.; Dumas, C. The crystal structure of HIV-1 Nef protein bound to the Fyn kinase SH3 domain suggests a role for this complex in altered T cell receptor signaling. *Structure* **1997**, *5*, 1361−1372.
(41) Lee, C. H.; Saksela, K.; Mirza, U. A.; Chait, B. T.; Kuriyan, J. Crystal structure of the conserved core of HIV-1 Nef complexed with a Src family SH3 domain. *Cell* **1996**, *85*, 931−942.
(42) Chan, B.; Lanyi, A.; Song, H. K.; Griesbach, J.; Simarro-Grande, M.; Poy, F.; Howie, D.; Sumegi, J.; Terhorst, C.; Eck, M. J. SAP couples Fyn to SLAM immune receptors. *Nat. Cell Biol.* **2003**, *5*, 155−160.
(43) Rieping, W.; Habeck, M.; Nilges, M. Inferential Structure Determination. *Science* **2005**, *309*, 303−306.
(44) Mulhern, T. D.; Shaw, G. L.; Morton, C. J.; Day, A. J.; Campbell, I. D. The SH2 domain from the tyrosine kinase Fyn in complex with a phosphotyrosyl peptide reveals insights into domain stability and binding specificity. *Structure* **1997**, *5*, 1313−1323.
(45) Arold, S. T.; Ulmer, T. S.; Mulhern, T. D.; Werner, J. M.; Ladbury, J. E.; Campbell, I. D.; Noble, M. E. The role of the Src homology 3-Src homology 2 interface in the regulation of Src kinases. *J. Biol. Chem.* **2001**, *276*, 17199−17205.
(46) Jelić, D.; Brandt, W. Three-dimensional structure of the Fyn tyrosine kinase deduced by homology modeling. Presented at the 8th Summer School on Biophysics, Rovinj, Croatia, Sep 14−26, 2003; P-105.
(47) Jelić, D.; Verbanac, D.; Koštrun, S.; Brandt, W. Fyn tyrosine kinase - 3-D structure and active site determination. Presented at the 7th MipTec, Basel, Switzerland, May 3−6, 2004; P-A135.
(48) Diller, D. J.; Li, R. Kinases, homology models, and high throughput docking. *J. Med. Chem.* **2003**, *46*, 4638−4647.
(49) Crowther, J. R. ELISA: Theory and practice. In *Methods in Molecular Biology*, 1st ed.; Vol. 42, Humana Press Inc.; Totowa, NJ, 1995.
(50) Anderoti, P. E.; Ludwig, G. V.; Peruski, A. H.; Tuite, J. J.; Morse, S. S.; Peruski, L. F., Jr. Immunoassay of infectious agents. *BioTechniques* **2003**, *35* (4), 850−859.
(51) Parker, G. J.; Law, T. L.; Lenoch, F. J.; Bolger, R. E. Development of High Throughput Screening Assays Using Fluorescence Polarization: Nuclear Receptor-Ligand-Binding and Kinase/Phosphatase Assays. *J. Biomol. Screening* **2000**, *5* (2), 77−88.
(52) Marangoni, A. G. *Enzyme kinetics—A Modern Approach*; Wiley-Interscience: New York, 2003.
(53) Semba, K.; Nishizawa, M.; Miyajima, N.; Yoshida, M. C.; Sukegawa, J.; Yamanashi, Y.; Sasaki, M.; Yamamoto, T.; Toyoshima, K. Yes-related protooncogene, syn, belongs to the protein-tyrosine kinase family. *Proc. Natl. Acad. Sci U.S.A.* **1986**, *83* (15), 5459−5463.
(54) Jelić, D.; Tóth, T.; Verbanac, D. Macromolecular Databases—a background of bioinformatics. *Food Technol. Biotechnol.* **2003**, *41* (3), 269−286.
(55) National Center for Biotechnology Information [http://www.ncbi.nlm.nih.gov].
(56) Xu, W.; Doshi, A.; Lei, M.; Eck, M. J.; Harrison, S. C. Crystal structures of c-Src reveal features of its autoinhibitory mechanism. *Mol. Cell* **1999**, *3*, 629−638.
(57) Williams, J. C.; Weijland, A.; Gonfloni, S.; Thompson, A.; Courtneidge, S. A.; Superti-Furga, G.; Wierenga, R. K. The 2.35 Å crystal structure of the inactivated form of chicken Src: a dynamic molecule with multiple regulatory interactions. *J. Mol. Biol.* **1997**, *274*, 757−775.
(58) Schindler, T.; Sicheri, F.; Pico, A.; Gazit, A.; Levitzki, A.; Kuriyan, J. Crystal structure of Hck in complex with a Src family-selective tyrosine kinase inhibitor. *Mol. Cell* **1999**, *3*, 639−648.
(59) Sicheri, F.; Moarefi, I.; Kuriyan, J. Crystal structure of the Src family tyrosine kinase Hck. *Nature* **1997**, *385*, 602−609.
(60) Berman, H. M.; Westbrook, J.; Feng, Z.; Gilliland, G.; Bhat, T. N.; Weissig, H.; Shindyalov, I. N.; Bourne, P. E. The Protein Data Bank. *Nucleic Acids Res.* **2000**, *28*, 235−242.
(61) Corpet, F. Multiple sequence alignment with hierarchical clustering. *Nucl. Acids Res.* **1988**, *16* (*22*), 10881−10890.
(62) Mittl, P. R.; Di Marco, S.; Krebs, J. F.; Bai, X.; Karanewsky, D. S.; Priestle, J. P.; Tomaselli, K. J.; Grutter, M. G. Structure of recombinant human CPP32 in complex with the tetrapeptide acetyl-Asp-Val-Ala-Asp fluoromethyl ketone. *J. Biol. Chem.* **1997**, *272*, 6539−6547.
(63) ExPASy (Expert Protein Analysis System) proteomics server of the Swiss Institute of Bioinformatics [http://www.expasy.org/].
(64) SYBYL, Tripos molecular modeling program package [http://www.tripos.com/data/SYBYL].
(65) Blundell, T.; Carney, D.; Gardner, S.; Hayes, F.; Howlin, B.; Hubbard, T.; Overington, J.; Singh, D. A.; Sibanda, B. L.; Sutcliffe, M. Knowledge-based protein modeling and design. *Eur J. Biochem.* **1988**, *172* (3), 513−20.
(66) Laskowski, R. A.; MacArthur, M. W.; Moss, D. S.; Thornton, J. M. Procheck: a program to check the stereochemical quality of protein structures. *J. Appl. Crystallogr.* **1993**, *26*, 283−291.
(67) Sippl, M. J. Recognition of errors in three-dimensional structures of proteins. *Proteins* **1993**, *17*, 355−362.
(68) Nolen, B.; Taylor, S.; Gourisankar, G. Regulation of Protein Kinases: Controlling Activity through Activation Segment Conformation. *Mol. Cell* **2004**, *15*, 661−675.
(69) Zhu, X.; Kim, J. L.; Newcomb, J. R.; Rose, P. E.; Stover, D. R.; Toledo, L. M.; Zhao, H.; Morgenstern, K. A. Structural analysis of the lymphocyte-specific kinase Lck in complex with non-selective and Src family selective kinase inhibitors. *Structure* **1999**, *7*, 651−661.
(70) Jones, G.; Willett, P.; Glen, R. C.; Leach, A. R.; Taylor, R. Development and validation of a genetic algorithm for flexible docking. *J. Mol. Biol.* **1997**, *267*, 727−748.
(71) Rarey, M.; Kramer, B.; Lengauer, T.; Klebe, G. A fast flexible docking method using an incremental construction algorithm. *J. Mol. Biol.* **1996**, *261*, 470−489.
(72) Feng, S.; Chen, J. K.; Yu, H.; Simon, J. A.; Schreiber, S. L. Two binding orientations for peptides to the Src SH3 domain: development of a general model for SH3-ligand interactions *Science* **1994**, *266* (5188), 1241−1247.
(73) Lamers, M. B.; Antson, A. A.; Hubbard, R. E.; Scott, R. K.; Williams, D. H. Structure of the protein tyrosine kinase domain of C-terminal Src kinase (CSK) in complex with staurosporine. *J. Mol. Biol.* **1999**, *285* (2), 713−25.
(74) Gadue, P.; Morton, N.; Stein, P. L. The Src family tyrosine kinase Fyn regulates natural killer T cell development. *J. Exp. Med.* **1999**, *190* (8), 1189−1196.
(75) Denny, M. F.; Patai, B.; Straus, D. B. Differential T-Cell Antigen Receptor Signaling Mediated by the Src Family Kinases Lck and Fyn. *Mol. Cell. Biol.* **2000**, *20* (4), 1426−1435.
(76) Schillace, R. V.; Scott, J. D. Organization of kinases, phosphatases, and receptor signaling complexes. *J. Clin. Invest.* **1999**, *103* (6), 761−765.
(77) Force, T.; Kuida, K.; Namchuk, M.; Parang, K.; Kyriakis, J. M. Inhibitors of Protein Kinase Signaling Pathways: Emerging Therapies for Cardiovascular Disease. *Circulation* **2004**, *109*, 1196−1205.
(78) Ho, G. J.; Drego, R.; Hakimian, E.; Masliah, E. Mechanisms of cell signaling and inflammation in Alzheimer's disease. *Curr. Drug Targets Inflamm. Allergy* **2005**, *4* (2), 247−56.
(79) Adcock, I. M.; Chung, K. F.; Caramori, G.; Ito, K. Kinase inhibitors and airway inflammation. *Eur. J. Pharm.* **2006**, *533*, 118−132.
(80) Congreve, M.; Murray, C. W.; Blundell, T. L. Structural biology and drug discovery. *Drug Discovery Today* **2005**, *10* (13), 895−907.
(81) Hardy, L. W.; Malikayil, A. The impact of structure-guided drug design on clinical agents. *Curr. Drug Discovery* **2003**, *12*, 15−20.

(82) Cornell, W. D.; Cieplak, P.; Bayly, C. I.; Gould, I. R.; Merz, K. M., Jr.; Ferguson, D. M.; Spellmeyer, D. C.; Fox, T.; Caldwell, J. W.; Kollman, P. A. A second generation force field for the simulation of proteins, nucleic acids and organic molecules. *J. Am. Chem. Soc.* **1995**, *117*, 5179−5197.

(83) Clark, M.; Cramer, R. D.; Van Opdenbosch, N. Validation of the General Purpose Tripos 5.2 Force Field. *J. Comput. Chem.* **1989**, *10*, 982−1012.

(84) Watts, J. D.; Wilson, G. M.; Ettenhadieh, E.; Clark-Lewis, I.; Kubanek, C. A.; Astell, C. R.; Marth, J. D.; Aebersold, R. J. Purification and initial characterization of the lymphocyte-specific protein-tyrosyl kinase p56lck from a baculovirus expression system. *Biol. Chem.* **1992**, *267* (2), 901−907.

(85) Ramer, S. E.; Winkler, D. G.; Carrera, A.; Roberts, T. M.; Walsh, C. T. Purification and initial characterization of the lymphoid-cell protein-tyrosine kinase p56lck from a baculovirus expression system. *Proc. Natl. Acad. Sci. U.S.A.* **1991**, *88* (14), 6254−6258.

(86) Koegl, M.; Kypta, R. M.; Bergman, M.; Alitalo, K.; Courtneidge, S. A. Rapid and efficient purification of Src homology 2 domain-containing proteins: Fyn, Csk and phosphatidylinositol 3-kinase p85. *Biochem. J.* **1994**, *302*, 737−744.

(87) Čalić, M.; Jelić, D.; Antolović, R.; Nujić, K.; Marjanović, N.; Stupin Polančec, D.; Vikić Topić, S.; Verbanac, D. Flavonoids as Inhibitors of Lck and Fyn Kinases. *Croat. Chem. Acta* **2005**, *78* (3), 367−374.

(88) Verbanac, D.; Jelić, D.; Stepanić, V.; Tatić, I.; Žiher, D.; Koštrun, S. Combined *in silico* and *in vitro* approach to drug screening. *Croat. Chem. Acta* **2005**, *78*, 133−139.

(89) Bovaird, J. H.; Ngo, T. T.; Lenhoff, H. M. Optimizing the o-phenylenediamine assay for horseradish peroxidase: effects of phosphate and pH, substate and enzyme concentrations, and stopping reagents. *Clin. Chem.* **1982**, *28* (12), 2423−2426.

JM0607202